

# Deformation effects in Giant Monopole Resonance

J Kvasil<sup>1</sup>, V O Nesterenko<sup>2</sup>, A Repko<sup>1</sup>, D Bozik<sup>1</sup>, W Kleinig<sup>2,3</sup> and P -G Reinhard<sup>4</sup>

<sup>1</sup> Institute of Particle and Nuclear Physics MFF UK, Charles University, CZ-18000 Prague 8, Czech Republic

<sup>2</sup> Laboratory of Theoretical Physics, Joint Institute for Nuclear Research, Dubna, Moscow region, 141980, Russia

<sup>3</sup> Technical University of Dresden, Institute for Analysis, D-01062, Dresden, Germany

<sup>4</sup> Institute of Theoretical Physics II, University of Erlangen, D-91058, Erlangen, Germany

E-mail: kvasil@ipnp.troja.mff.cuni.cz

**Abstract.** The isoscalar giant monopole resonance (GMR) in Samarium isotopes (from spherical  $^{144}\text{Sm}$  to deformed  $^{148-154}\text{Sm}$ ) is investigated within the Skyrme random-phase-approximation (RPA) for a variety of Skyrme forces. The exact RPA and its separable version (SRPA) are used for spherical and deformed nuclei, respectively. The quadrupole deformation is shown to yield two effects: the GMR broadens and attains a two-peak structure due to the coupling with the quadrupole giant resonance.

## 1. Introduction

During last decades, the GMR remains to be a subject on intense studies (see [1, 2, 3] for recent reviews and discussions) as it provides a valuable information on the nuclear incompressibility [4]. Unlike early explorations, the present theoretical analysis is mainly done within the self-consistent mean field models (SC-MFM) [5, 6], in particular those based on Skyrme forces [5, 7, 8, 9]. A variety of experimental data becomes available, see e.g. [10, 11, 12, 13, 14, 15].

Despite an impressive theoretical and experimental effort, some GMR problems are not yet resolved. For example, the GMR experimental data in spherical nuclei, Sn/Cd isotopes [11, 12] from one side and Pb/Sm isotopes [13, 14] from another side, cannot be simultaneously reproduced by any SC-MFM [1, 2, 17, 18, 19]. It is not yet clear if this is caused by a poor theoretical description (e.g., too rough treatment of the pairing impact [16, 17, 18, 19]) or by a lack of accuracy of experimental data [10, 11, 12, 13, 14, 15]. Note that two main experimental group measuring GMR in  $(\alpha, \alpha')$  reaction, Texas A&M University (TAMU) [13, 15] and Research Center for Nuclear Physics (RCNP) at Osaka University [10, 11, 14], indeed sometimes provide noticeably different results.

The situation with GMR in deformed nuclei is even more vague. Though there is an evident progress in experiment studies, e.g. for soft Mo [15] and deformed Sm [10, 13] isotopes, the SC-MFM calculations are yet at very beginning, which is explained by a need to deal with a huge configuration space. So the theoretical results on GMR in deformed nuclei are now mainly reduced to early inconsistent studies based on phenomenological mean fields [20, 21, 22]. More than three decades ago, two deformation effects have been predicted [20, 21, 22] and observed [23, 24] in GMR: i) broadening the resonance and ii) onset of two-peak structure due to a

coupling with the  $\mu = 0$  branch of the giant quadrupole resonance (GQR). Obviously it is worth to revisit these results by using a modern theoretical framework, e.g. the Skyrme SC-MFM. This is just the aim of the present study.

We consider GMR in a chain of Sm isotopes, from spherical  $^{144}\text{Sm}$  to deformed  $^{154}\text{Sm}$ , within the Skyrme random-phase approximation (RPA) approach. For spherical nuclei, the exact RPA method [25] is used. For deformed nuclei, the separable RPA (SRPA) [26, 27] is implemented. This method exploits the self-consistent factorization of the residual interaction, which drastically decreases the computational effort while keeping high accuracy of the calculations. SRPA was proved as very reliable and effective theoretical tool in investigation of various electric [28, 29, 30] and magnetic [31] giant resonances in both axially deformed and spherical nuclei. In particular, SRPA was used for exploration of the impact of the time-odd current density on the properties of GMR in  $^{208}\text{Pb}$  [30]. In spherical nuclei, SRPA and exact RPA results are about identical. Both methods are fully self-consistent.

The calculations employ a wide set of Skyrme forces with various isoscalar effective masses  $m_0/m$ : SkT6 [32], SVbas [33], SkM\*[34], SGII [35], SLy6 [36] and SkI3 [37].

## 2. Theoretical framework

The calculations are performed within exact RPA [25] for spherical  $^{144}\text{Sm}$  and SRPA [26, 27] for soft and axially deformed  $^{148,150,152,154}\text{Sm}$ . For every nucleus, the equilibrium deformation  $\beta_2$  is determined. Then, for the isoscalar monopole transition operator  $\hat{M} = \sum_i^A (r^2 Y_{00})_i$ , the strength function

$$S(E0; E) = \sum_{\nu} E_{\nu} |\langle \nu | \hat{M} | 0 \rangle|^2 \xi_{\Delta}(E - E_{\nu}) \quad (1)$$

with the Lorentz weight  $\xi_{\Delta}(E - E_{\nu}) = \frac{1}{2\pi} \frac{\Delta}{(E - E_{\nu})^2 - \Delta^2/4}$  is computed. Here,  $|0\rangle$  is the ground state wave function,  $|\nu\rangle$  and  $E_{\nu}$  are RPA states and energies,  $\Delta$  is the averaging parameter. The Lorentz weight roughly simulates smoothing effects beyond RPA (coupling to complex configurations and escape widths) and allows a convenient comparison of the calculated and experimental strengths. In the present study, the averaging  $\Delta = 2$  MeV is found optimal. Note that the same averaging was used for the giant dipole resonance [28].

In SRPA calculations for deformed nuclei, the input (doorway) operators  $r^2 Y_{00}$ ,  $r^4 Y_{00}$ ,  $j_0(qr) Y_{00}$  (with  $q=0.4, 0.6$ ) and  $r^2 Y_{20}$  are used. Following the standard SRPA procedure [26, 27], the first operator is the transition one. This operator favors surface excitations. Then some next operators (with higher power and Bessel-function radial dependence) are added to take into account the nuclear interior motion. Finally the quadrupole operator is included to take into account the coupling to quadrupole excitations (to be omitted in spherical nuclei). At 5 input operators, the rank of the SRPA matrix is  $5 \times 4$ , which is much less than a huge rank of conventional RPA matrices. As seen from Fig. 1, the set with 4 operators provides an excellent agreement between SRPA and exact RPA results in spherical  $^{144}\text{Sm}$ .

In SRPA calculations for  $^{148-152}\text{Sm}$ , the pairing  $\delta$ -force

$$V_{pair}(\vec{r}, \vec{r}') = V_0 \left[ 1 - \eta \left( \frac{\rho(\vec{r})}{\rho_0} \right)^{\gamma} \right] \delta(\vec{r} - \vec{r}') \quad (2)$$

is used at the BCS level [38]. For SVbas, both volume ( $\eta = 0$ ) and density-dependent surface ( $\eta = 1$ ) pairing options are used. Other Skyrme forces exploit the standard volume pairing.

The calculations use a large configuration space with particle-hole (two-quasiparticle) energies up to 70-75 MeV. For the force SVbas, the monopole strength summed at the relevant energy interval 9-45 MeV exhausts the energy weighted sum rule EWSR =  $\frac{\hbar^2}{2\pi m} A \langle r^2 \rangle_0$  by 100-105%, depending on the isotope. The similar results are for other forces. The spurious mode lies at 2-7 MeV, i.e. safely below the GMR concentrated at 10-20 MeV.

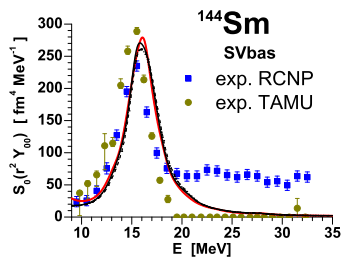


**Figure 1.** E0 strength function in the spherical  $^{144}\text{Sm}$  calculated within full RPA (thick red line) and SRPA (black lines). In SRPA, the input operators  $f(r)Y_{00}$  with radial dependence  $r^2$  (dotted line),  $r^2, r^4$  (dashed line) and  $r^2, r^4, j_0(0.4r), j_0(0.6r)$  (thin line) are used. The RCNP [10] and TAMU [13] experimental data are depicted.

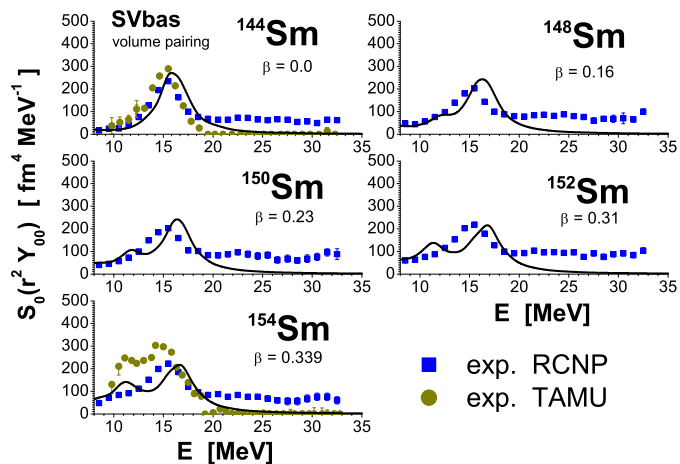


**Figure 2.** E0 strength functions in Sm isotopes, calculated with SVbas force within full RPA ( $^{144}\text{Sm}$ ) and SRPA ( $^{148-154}\text{Sm}$ ), as compared to RCNP [10] and TAMU [13] experimental data. For every isotope, the deformation parameter  $\beta_2$  is shown.

### 3. Results and discussion

In Figure 1, the E0 strengths calculated within full RPA and SRPA (with different sets of input operators) are compared. It is seen that RPA and SRPA strengths are about identical already for one input operator  $r^2 Y_{00}$ , which indicates a high accuracy of SRPA. This is partly caused by a simple one-peak form of the GMR. Next three SRPA input operators are almost irrelevant here. However, following our calculations, they are necessary for description of a more complicated GMR form in deformed nuclei.

Figure 1, as well as next figures, exhibit the RCNP [10] and TAMU [13] experimental data. For convenience of the comparison, the TAMU data, being initially presented in units of the EWSR/E (where EWSR is the energy-weighted sum rule given in Sec. 2 and E is the excitation energy), are transformed to units  $\text{fm}^4 \text{MeV}^{-1}$  used in RCNP. Following Fig. 1, the RCNP and TAMU data give about the same GMR peak energy but considerably deviate at energies above the GMR location, i.e. at  $E > 19$  MeV. Namely, RCNP indicates a large and about uniform tail of E0 strength at  $19 \text{ MeV} < E < 33 \text{ MeV}$  while TAMU gives here a vanishing strength (see critical discussion of this discrepancy in [13]). This difference can affect determination of experimental GMR energy centroids which are usually estimated through evaluation of sum rules with different energy weights and thus depend on the chosen energy interval.

As seen from Fig. 1, both full RPA and SRPA results well reproduce the peak energy and width of the GMR (though the later is mainly attributed to the proper choice of the average parameter  $\Delta=2$  MeV). For  $E > 19$  MeV, our calculations, in agreement to TAMU data [13], do not give any significant tail.

In Figure 2, the full RPA and SRPA results obtained with the force SVbas are compared to TAMU [13] and RCNP [10] data for the set of Sm isotopes. Parameters of the equilibrium quadrupole deformation  $\beta_2$  determined from the minimum of the nuclear energy show that only  $^{144}\text{Sm}$  is spherical while other isotopes are soft ( $^{148}\text{Sm}$ ) or well deformed ( $^{150-154}\text{Sm}$ ). The E0 strength is calculated within full RPA in  $^{144}\text{Sm}$  and SRPA in  $^{148-154}\text{Sm}$  (with 5 input operators as discussed above). It is seen that our calculations well reproduce broadening of the

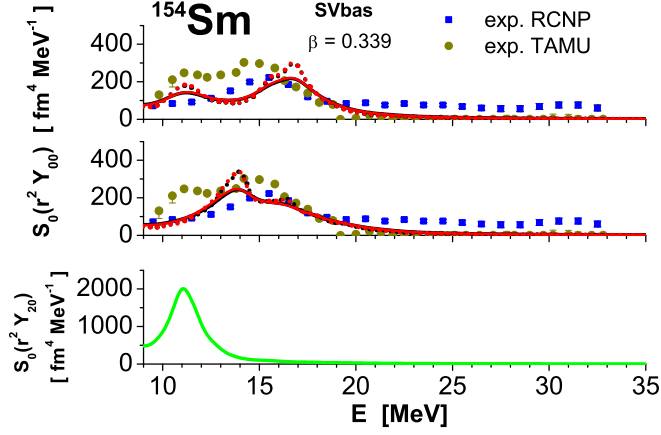


**Figure 3.** Isoscalar E0 (upper and middle panels) and E2 (bottom panel) strength functions in deformed  $^{154}\text{Sm}$  calculated within SRPA with the force SVbas. The E0 strength is determined with (upper panel) and without (middle panel) coupling to the quadrupole excitations. The E0 results obtained with the volume (black curves) and surface (red curves) pairing as well as with the averaging  $\Delta=1$  MeV (dotted curves) and 2 MeV (solid curves), are compared. The RCNP [10] and TAMU [13] experimental data are shown.

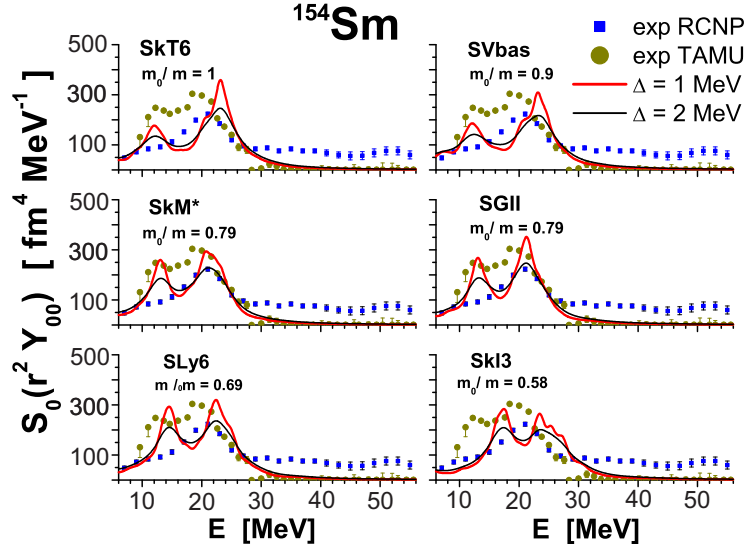


**Figure 4.** Isoscalar E0 strengths in  $^{154}\text{Sm}$ , calculated for different Skyrme parametrizations (SkT6, SVbas, SkM\*, SGII, SLy6 and SkI3) and two values of the Lorentz averaging parameter,  $\Delta = 1$  and 2 MeV, as compared to TAMU [13] and RCNP [10] experimental data. For each force, the isoscalar effective mass  $m_0/m$  is shown.

GMR and onset of the GMR two-peak structure with growth of the deformation from  $^{144}\text{Sm}$  to  $^{154}\text{Sm}$ . The latter effect is caused by the coupling of E0 and E2 modes in deformed nuclei [20, 21, 22, 23, 24]. Note that the two-peak structure in deformed Sm isotopes is observed in TAMU [13] but not in RCNP [10] experiments, which ones more signals on the essential difference between measurements of these two groups.

The origin of the two-peak structure is demonstrated in Fig. 3 for  $^{154}\text{Sm}$ . It is seen that the first peak takes place if E0-E2 coupling is included through the input operator  $r^2Y_{20}$  (upper plot) but is absent if the coupling is switched off (middle plot). Moreover, the position of the first peak in E0 strength coincides with position of  $\mu = 0$  branch of the quadrupole resonance, exhibited at the bottom plot. The upper and middle plots also show sensitivity of the results to the choice of pairing (volume vs surface) and average parameter  $\Delta$  (1 or 2 MeV). Though these factors somewhat change the results, the qualitative picture remains the same.

Finally in Fig.4, the GMR calculated in  $^{154}\text{Sm}$  with different Skyrme forces is shown. It is seen that the first GMR peak is generally upshifted with decreasing the isoscalar effective mass  $m_0/m$ . The better agreement is obtained for the forces with a large  $m_0/m$ , from SkT6 to SGII. All the Skyrme forces give the two-peak GMR structure. Our results for E0 strength at the GMR region and above are in a general agreement with TAMU [13] data and do not correspond to RCNP [10] distributions. The results with  $\Delta=1$  and 2 MeV look qualitatively similar though the larger averaging is more convenient for the comparison to experiment. It is remarkable that changing  $\Delta$  from 1 to 2 MeV practically does not affect the description of the GMR width in deformed nuclei. The same was found for the giant dipole resonance [28].

#### 4. Conclusions

The GMR in Sm isotopes, from spherical  $^{144}\text{Sm}$  to deformed  $^{148-154}\text{Sm}$ , was explored. We used exact RPA [25] for spherical  $^{144}\text{Sm}$  and separable RPA (SRPA) [26, 27] for deformed isotopes (both methods are fully self-consistent). Various Skyrme forces (SkT6, SVbas, SkM, SGII, SLy6 and SkI3) were involved. The SRPA calculations have shown distinct deformation effects: i) broadening the GMR and ii) splitting of the resonance into two peaks. The latter effect was shown to be caused by the coupling between GMR and  $\mu=0$  branch of the quadrupole giant resonance. The obtained results are in a good agreement with TAMU experimental data [13] which support the two-peak GMR structure. At the same time, they deviate from RCNP [10] data which exhibit a one-bump GMR structure and an impressive high-energy distribution of E0 strength. Certainly, further exploration of GMR in Sm isotopes needs a harmonization of available experimental data.

The calculations with different Skyrme forces give rather close results though the forces with a large isoscalar effective mass  $m_0/m$  (from SkT6 to SGII) look more promising. In accordance to previous studies, the volume and surface pairings give similar effects in GMR.

#### Acknowledgments

The work was partly supported by the DFG grant RE 322/14-1, Heisenberg-Landau (Germany-BLTP JINR), and Votruba-Blokhincev (Czech Republic-BLTP JINR) grants. P.-G.R. and W.K. are grateful for the BMBF support under the contracts 05P12RFFTG and 05P12ODDUE, respectively. The support of the Czech Science Foundation (P203-13-07117S) is appreciated.

#### References

- [1] Coló G 2008 *Phys. Part. Nucl.* **39** 286.
- [2] Avogadro P and Bertulani C A 2013 *Phys. Rev.* **C88** 044319.
- [3] Stone J R, Stone N J and Moszkowski S A 2014 arXiv: 1404.0744 [nucl-th].
- [4] Blaizot J 1980 *Phys. Rep.* **64** 171
- [5] Bender M, Heenen P-H and Reinhard P-G, 2003 *Rev. Mod. Phys.* **75** 121.
- [6] Vretenar D, Afanasjev A V, Lalazissis G A and Ring P 2005 *Phys. Rep.* **409** 101.
- [7] Skyrme T H R 1956 *Phil. Mag.* **1** 1043.
- [8] Vauterin D and Brink D M 1972 *Phys. Rev.* **C5** 626.
- [9] Engel Y M et al 1975 *Nucl. Phys.* **A249** 215.
- [10] Itoh M, et al. 2003 *Phys. Rev.* **C68** 064602
- [11] Li T, et al. 2012 *Phys. Rev.* **C99** 162503

- [12] Patel D, et al. 2012 *Phys. Letters* **B718** 447
- [13] Youngblood D H et al 2004 *Phys. Rev.* **C69** 034315
- [14] Uchida M, et al. 2004 *Phys. Rev.* **C69** 051301(R)
- [15] Youngblood D H et al 2013 *Phys. Rev.* **C88** 021301(R)
- [16] Khan E 2009 *Phys. Rev. C* **80** 011307R; *ibid* **80** 057302.
- [17] Vesely P, Toivanen J, Carlsson B C, Dobaczewski J, Michel M and Pastore D 2012 *Phys. Rev.* **C86** 024303
- [18] Cao L, Sagawa H and Colo G 2012 *Phys. Rev.* **C86** 054313
- [19] Avogadro P and Nakatsukasa T 2013 *Phys. Rev.* **C87** 014331
- [20] Kishimoto T 1975 *Phys. Rev. Lett.* **35** 552.
- [21] Zawischa D, Speth J and Pal D 1978 *Nucl. Phys.* **bf A311** 445.
- [22] Abgrall Y, Morand B, Caurier E and Grammaticos N 1980 *Nucl. Phys.* **A346** 431.
- [23] Buender M et al 1980 *Phys. Rev. Lett.* **45** 1667.
- [24] Garg U et al 1984 *Phys. Rev.* **C29** 93.
- [25] Repko A, Kvasil J, Nesterenko V O and Reinhard P-G (under preparation for publication).
- [26] Nesterenko V O, Kvasil J, Reinhard P -G (2002) *Phys. Rev.* **C66** 044307.
- [27] Nesterenko V O, Kleinig W, Kvasil J, Vesely P, Reinhard P-G and Dolci D S 2006 *Phys. Rev.* **C74** 064306.
- [28] Kleinig W, Nesterenko V O, Kvasil J, Reinhard P-G and Vesely P 2008 *Phys. Rev.* **C78** 044313.
- [29] Kvasil J, Nesterenko V O, Kleinig W and Reinhard P-G 2014 *Phys. Scr.* **89** 054023.
- [30] Nesterenko V O, Kleinig W, Kvasil J, Vesely P and Reinhard P-G 2007 *Proceed. of 26th Intern. Workshop on Nucl. Theory (Rila, Bulgaria, 2007)* ed. S. Dimitrova (INRNE BAS, 2007) p. 273.
- [31] Vesely P, Kvasil J, Nesterenko V O, Kleinig W, Reinhard P-G and Ponomarev V Yu 2009 *Phys. Rev.* **C80** 031302.
- [32] Tondeur F, Brack M, Farine M and Pearson J M 1984 *Nucl. Phys.* **A420** 297.
- [33] Kluepfel P, Reinhard P-G, Buervenich T J and Maruhn J A 2009 *Phys. Rev. C* **79** 034310.
- [34] Bartel J, Quentin P, Brack M, Guet C and Haakansson H-B 1982 *Nucl. Phys. A* **386** 79.
- [35] Van Giai N and Sagawa H 1981 *Phys. Lett.* **B106** 379.
- [36] Chabanat E, Bonche P, Haensel P, Meyer J and Schaeffer R 1997 *Nucl. Phys. A* **627** 710.
- [37] Reinhard P-G and Flocard F 1995 *Nucl. Phys.* **A584** 467.
- [38] Bender M, Rutz K, Reinhard P-G and Maruhn J A 2000 *Eur. Phys. J. A* **8** 59.